

# Phosphodiesterase III inhibition promotes differentiation and survival of oligodendrocyte progenitors and enhances regeneration of ischemic white matter lesions in the adult mammalian brain

Nobukazu Miyamoto<sup>1</sup>, Ryota Tanaka<sup>1,2</sup>, Hideki Shimura<sup>1,2</sup>, Terubumi Watanabe<sup>1</sup>, Hideo Mori<sup>1,3</sup>, Masafumi Onodera<sup>4</sup>, Hideki Mochizuki<sup>1</sup>, Nobutaka Hattori<sup>1</sup> and Takao Urabe<sup>1</sup>

<sup>1</sup>Department of Neurology, Juntendo University School of Medicine, Tokyo, Japan; <sup>2</sup>Department of Neurology, Juntendo University Urayasu Hospital, Chiba, Japan; <sup>3</sup>Department of Neurology, Juntendo Koshigaya Hospital, Saitama, Japan; <sup>4</sup>Laboratory of Genetic Diagnosis and Gene Therapy Department of Genetics National Research Institute for Child Health and Development, Tokyo, Japan

**Vascular dementia is caused by blockage of blood supply to the brain, which causes ischemia and subsequent lesions primarily in the white matter, a key characteristic of the disease. In this study, we used a chronic cerebral hypoperfusion rat model to show that the regeneration of white matter damaged by hypoperfusion is enhanced by inhibiting phosphodiesterase III. A rat model of chronic cerebral hypoperfusion was prepared by bilateral common carotid artery ligation. Performance at the Morris water-maze task, immunohistochemistry for bromodeoxyuridine, as well as serial neuronal and glial markers were analyzed until 28 days after hypoperfusion. There was a significant increase in the number of oligodendrocyte progenitor cells in the brains of patients with vascular dementia as well as in rats with cerebral hypoperfusion. The oligodendrocyte progenitor cells subsequently underwent cell death and the number of oligodendrocytes decreased. In the rat model, treatment with a phosphodiesterase III inhibitor prevented cell death, markedly increased the mature oligodendrocytes, and promoted restoration of white matter and recovery of cognitive decline. These effects were cancelled by using protein kinase A/C inhibitor in the phosphodiesterase III inhibitor group. The results of our study indicate that the mammalian brain white matter tissue has the capacity to regenerate after ischemic injury.**

*Journal of Cerebral Blood Flow & Metabolism* (2010) **30**, 299–310; doi:10.1038/jcbfm.2009.210; published online 14 October 2009

**Keywords:** chronic cerebral hypoperfusion; ischemic white matter disease; oligodendrocyte progenitor cell; phosphodiesterase III inhibitor; regenerative therapy

## Introduction

Cerebrovascular disease is one of the major causes of death in the world, and there are only a few effective

clinical treatments that enhance recovery. Furthermore, the number of patients afflicted with cerebral infarction is increasing, and stroke is a leading cause of disability. Cognitive decline and depressive disorders are well-recognized complications in poststroke patients. Brain white matter lesions, which are often observed in patients with ischemic cerebrovascular diseases, contribute to cognitive decline. White matter damage, including loss of oligodendrocytes, myelin and axonal damage (a hallmark of vascular dementia), and ischemic cerebrovascular disease, can be induced experimentally by permanently occluding the common carotid artery of rats to cause chronic cerebral ischemia. This experimental model is considered suitable for investigations of vascular dementia and cerebrovascular white matter disease (Ihara *et al*, 2001; Wakita *et al*, 1994).

Correspondence: Dr R Tanaka, Department of Neurology, Juntendo University School of Medicine, 2-1-1 Hongo, Bunkyo-ku, Tokyo 113-0033, Japan.

E-mail: r\_tanaka@juntendo.ac.jp

This study was supported in part by a High Technology Research Center grant and a Grant-in-Aid for Exploratory Research from the Ministry of Education, Culture, Sports, Science and Technology, Japan. This study was supported by Grant-in-Aid for Scientific Research (Young Scientists B) of the Ministry of Education, Culture, Sports, Science and Technology (MEXT).

Received 13 August 2009; revised 9 September 2009; accepted 10 September 2009; published online 14 October 2009

The myelin membrane that ensheathes axons in the central nervous system (CNS) is produced by oligodendrocytes and functions to increase the rate and efficiency of nerve conduction. Inadequate myelination or damage to the myelin sheaths, such as in ischemic cerebrovascular disease and multiple sclerosis, leads to severe neurologic deficits. Before myelin formation, oligodendrocyte progenitor cells (OPCs) progress through well-defined stages of a highly regulated developmental lineage, during which they undergo proliferation, migration, differentiation, and myelin membrane formation (Bansal and Pfeiffer, 1997). Even after the CNS development, OPCs are present in the adult CNS (Reynolds and Hardy, 1997; Wolswijk and Noble, 1989), and in response to demyelination, OPCs proliferate, migrate, rapidly fill the demyelinated area, and then differentiate into mature oligodendrocytes forming and restoring the new myelin sheaths (Gensert and Goldman, 1997; Redwine and Armstrong, 1998).

The presence of OPCs in the mature brain may provide the opportunity for significant renewal of oligodendroglial numbers after injury. Proliferation of OPCs at the margin of an infarct has been reported to occur between 1 and 7 days after ischemia, and increased numbers of those cells were detected both in the gray matter around the infarct and in the corpus callosum adjacent to the lesion (Mabuchi *et al*, 2000). Oligodendrocyte progenitor cells have been suggested to respond to a short, sublethal ischemic injury that causes myelin damage (Liu *et al*, 2001). Proliferation of OPCs is also reported to occur at the margins of infarcts 2 weeks after ischemia, and is considered to constitute an attempt to remyelinate the peri-infarct tissue (Tanaka *et al*, 2001). However, there are only limited data on regeneration of oligodendrocytes and tissue repair of ischemic white matter lesions of the mammalian CNS.

Cilostazol is a type III phosphodiesterase inhibitor (PDE3I) that has been approved for the treatment of intermittent claudication and improves pain-free walking distance in patients with peripheral arterial disease (Barnett *et al*, 2004), through improvement in endothelial dysfunction and reduction in platelet aggregation. Efficacy data from the Cilostazol Stroke Prevention Study support the use of cilostazol for secondary prevention of cerebral infarction, and the drug has been approved in Japan for clinical use in patients with stroke (Matsumoto, 2005). In addition to clinical use, PDE3I has anticytotoxic and anti-apoptotic effects in animal models of focal cerebral ischemia (Choi *et al*, 2002).

We have shown previously the beneficial effects of PDE3I on white matter lesions of rats after bilateral common carotid artery ligation (BCCAL) (Watanabe *et al*, 2006). In that study, we also reported an increase in oligodendrocytes in white matter lesions. Furthermore, another recent study has shown that inhibition of PDE3 promotes the generation of new neurons in the adult rodent CNS (Lee *et al*, 2009). This study was designed to assess the regenerative

capacity of ischemically degenerated white matter in rats induced by permanent occlusion of bilateral common carotid arteries. We also tested the hypothesis that inhibition of phosphodiesterase III promotes the generation of new oligodendrocytes and helps to restore the damaged white matter with subsequent recovery of cognitive decline. In addition to animal experiments, we also analyzed the pathologic and regenerative processes in brain white matter lesions of patients diagnosed with vascular dementia.

## Materials and methods

### Autopsy Specimens

We studied formalin-fixed paraffin-embedded sections of five patients with ischemic white matter disease and six normal control brain samples available at the Juntendo University. The average postmortem interval required for embedding the diseased tissue was 48 h. Some specimens were obtained as early as 2 to 6 h postmortem, and the fixation time was more than 2 weeks for all specimens. Multiple paraffin-embedded tissue blocks were prepared, 10- $\mu$ m-thick sections were cut, stained with Klüver–Barrera (KB) stain, and used for immunohistochemical analysis. The diagnosis was based on fulfilling the clinical diagnostic criteria for vascular dementia using Neurological Disorders and Stroke-Association Internationale pour la Recherche et l'Enseignement en Neurosciences (NINDS-AIREN) (Roman *et al*, 1993). The pathologic diagnosis made by a neuropathologist was multiinfarct dementia or Binswanger type dementia. The autopsies were conducted after obtaining informed consent from the relatives of deceased individuals.

### Experimental Studies

All animal procedures were approved by the Animal Care Committee of the Juntendo University. Adult male Wister rats (9 weeks of age and weighing 250 to 270 g) were purchased from Charles River Institute (Kanagawa, Japan) and maintained on a 12 light:12 dark cycle with free access to food and water. The rats were randomly divided into three groups. Rats of the first group (vehicle group,  $n=60$ ) underwent BCCAL but were provided normal animal food. Those of the second group (PDE3I-treated group,  $n=60$ ) underwent BCCAL but were provided food mixed with 0.1% cilostazol (50 mg/kg per day; Otsuka Pharmaceutical, Tokyo, Japan). After 7 days, the plasma cilostazol concentration was  $>0.1 \mu\text{mol/L}$ , which is sufficient to inhibit PDE III as determined by *in vitro*  $\text{IC}_{50}$  potency data. Similar cilostazol plasma concentrations were achieved up to 28 days after hypoperfusion in PDE3I-treated rats (plasma cilostazol at day 7,  $1.65 \pm 0.91 \mu\text{mol/L}$ ; at day 14,  $1.43 \pm 0.90 \mu\text{mol/L}$ ; at day 21,  $2.62 \pm 1.36 \mu\text{mol/L}$ ; at day 28,  $0.66 \pm 0.19 \mu\text{mol/L}$ ; no statistical differences,  $n=6$  in each group). Rats of the third group (sham-operated group,  $n=60$ ) neither underwent BCCAL nor received cilostazol.

Chronic cerebral hypoperfusion was induced by bilateral occlusion of the common carotid arteries using the method described previously (Wakita *et al*, 1994). Briefly, for

bilateral occlusion of the common carotid arteries, anesthesia was induced with 1.0% to 2.0% isoflurane in 30% oxygen and maintained during operation by administration of 70% nitrogen. Through a midline incision, the left and right common carotid arteries were carefully separated from the cervical sympathetic and vagal nerves, and ligated permanently. During this procedure, the body temperature was kept at  $37.0 \pm 0.5^\circ\text{C}$  using a heating pad (Unique Medical, Tokyo, Japan). Rats of each group were sacrificed at 7, 14, 21, or 28 days after BCCAL. Cerebral blood flow (CBF) was measured in left and right temporal windows by laser-Doppler flowmetry (Omega Wave, Tokyo, Japan) before operation and after BCCAL, as well as before sacrifice. Rats of each group were anesthetized with diethyl ether before transcatheterial perfusion. The brain was removed immediately *en bloc* and postfixed for 48 h in 4% paraformaldehyde in phosphate-buffered saline at  $4^\circ\text{C}$  before cryoprotection by bathing in 30% sucrose. The brain was then frozen and 20- $\mu\text{m}$ -thick consecutive coronal sections of the white matter were prepared on a cryostat (CM 1900, Leica Instruments, Nussloch, Germany). Serial sections were stained using the KB method. The severity of white matter lesions was assessed by the criteria defined by Wakita *et al* (1994, 1999).

### 5-Bromodeoxyuridine Labeling

To determine the phenotype of newly generated cells, 5-bromodeoxyuridine (BrdU), a cell proliferation marker, (Sigma-Aldrich, St Louis, MO, USA), was dissolved in saline and then injected intraperitoneally (50 mg/kg) thrice at 4-h intervals during the day. Two patterns of BrdU injection were used in relation to the time of sacrifice after BCCAL (Supplementary Figure 1A). 5-Bromodeoxyuridine was injected on the day of sacrifice (each group,  $n = 5$ ). In each group, the rats were sacrificed within 2 h of the last BrdU injection. Moreover, BrdU was also injected at 14 days after BCCAL and the survival rate was determined between the period of 14 and 21 days (14  $\rightarrow$  21d,  $n = 5$ ).

### Injection of Retroviral Vector into the White Matter

Rats were anesthetized with pentobarbital (45 mg/kg body weight, intraperitoneally), and the retroviral vector with improved enhanced green fluorescent protein (EGFP) expression (as described previously by Suzuki *et al* (2002)) was infused (2  $\mu\text{L}$  at 0.4  $\mu\text{L}/\text{min}$ ) into the right white matter (relative to the bregma: anterior, 0.4 mm; lateral, 1.7 mm; ventral, 2.8 mm; and tooth bar,  $-3$  mm). The animals underwent BCCAL at 72 h after viral injection.

### Intraventricular Infusion of Protein Kinase A and Protein Kinase C Inhibitor

An osmotic mini pump (infusion rate; 10 nmol/ $\mu\text{L}$  per h, Alzet; Durect Corporation, Cupertino, CA, USA) was filled with diluted H7 (Sigma-Aldrich) or control saline and connected to a brain infusion cannula (28 gauge, 5.0 mm height, Alzet). On day 7 after BCCAL, PDE3I-group rats ( $n = 5$ ) were anesthetized with 45 mg/mL pentobarbital, the

sterile brain-infusion cannula was stereotaxically implanted into the right lateral ventricle (from the bregma: posterior, 0.28 mm; lateral, 1.5 mm; and ventral, 4.5 mm; and tooth bar =  $-3$  mm), and fixed with dental cement. We also used BrdU labeling on the day the pump began operating to determine the survival rate of newly generated cells.

### Water-Maze Task

The water-maze task was performed to evaluate BCCAL-related learning deficits, using the method described by Gerlai (2001). The task was videotaped using a Victor camera (Everio GZ-MG-77-S, Victor Company of Japan, Limited, Yokohama, Japan) and analyzed. Tests were conducted on 3 consecutive days before, and at 7, 14, 21, and 28 days after BCCAL.

### Cyclic Adenosine Monophosphate Assay

Each brain white matter sample was rapidly removed at 7, 14, 21, and 28 days after BCCAL. The samples were lysed in CellLytic reagent (Sigma-Aldrich) with protease inhibitor (Calbiochem, La Jolla, CA, USA). The contents of cyclic adenosine monophosphate (cAMP) in the homogenized brain extracts were measured using immunoassay kits (R&D Systems, Minneapolis, MN, USA) as described previously (Choi *et al*, 2002).

### Immunohistochemistry

After incubation in 3%  $\text{H}_2\text{O}_2$  followed by 10% normal goat or horse serum (Dako Corporation, Carpinteria, CA, USA), the brain sections were immunostained overnight at  $4^\circ\text{C}$  using anti-glutathione-S-transferase pi (GST-pi, 1:500, Chemicon International, Temecula, CA, USA), antiplatelet-derived growth factor receptor- $\alpha$  (1:250, Santa Cruz Biotechnology, Santa Cruz, CA, USA), anti-ssDNA (1:250, Dako), anti-2', 3'-cyclic nucleotide 3'-phosphodiesterase (CNPase, 1:200), antigial fibrillary acidic protein (GFAP, dilution, 1:500; Dako), antiionized calcium binding adapter molecule-1 (Iba-1, dilution, 500:1, Wako Pure Chemical Industries, Osaka, Japan), phosphorylated form of cAMP response element-binding protein (pCREB, dilution, 1:100, Upstate Biotechnology, Lake Placid, NY, USA) and anti-PCNA (proliferating cell nuclear antigen) (1:50, Dako), and finally treated with secondary antibodies (1:500, Vectastain; Vector Laboratories, Burlingame, CA, USA). Immunoreactivity was visualized using the avidin-biotin complex method (Vectastatin). Negative control sections were stained using the above-mentioned immunohistochemical technique with the omission of the primary antibodies. The images were captured using a digital camera (DXM1200, Nikon, Tokyo, Japan) attached to an Olympus CX40 microscope (Olympus, Tokyo, Japan) and analyzed using the ACT-1 image system (version 2.20, Nikon).

### Immunofluorescence Histochemistry

Brain sections were incubated at  $68^\circ\text{C}$  for 30 mins in 1N HCl to detect BrdU labeling. The antigen-retrieval method

was used for myelin basic protein immunostaining. Briefly, the sections were heated to boiling point in 10 mmol/L sodium citrate buffer (pH 6.0) and maintained at a subboiling temperature for 5 mins. Sections were incubated overnight with anti-BrdU (1:50; Oxford Biotechnology, Oxford, UK). Double immunofluorescence staining was performed by simultaneously incubating the sections overnight at 4°C with anti-GST-pi (1:500), anti-CNPase (1:200), anti-NG2 (1:25; Santa Cruz Biotechnology), anti-PDGFR- $\alpha$  (1:200), anti-ssDNA (1:250), anti-PCNA (1:50), antimyelin basic protein (1:25; Chemicon International), antiphosphodiesterase 3B (PDE3B, 1:25; Santa Cruz Biotechnology), anti-CD31 (dilution, 1:100, BD Transduction Laboratories, Franklin Lakes, NJ, USA), pCREB (dilution, 1:100, Upstate Biotechnology), anti-GFP (1:100, Chemicon International), and anti-GFAP (1:500, Dako) antibody. For double labeling, primary antibodies were detected with Cy3- or fluorescein isothiocyanate-conjugated secondary antibody (1:500; Jackson ImmunoResearch Laboratories, West Grove, PA, USA) after incubation for 1 h at room temperature.

### Cell Counts and Statistical Analysis

An investigator blinded to the experimental groups counted the number of stained cells in white matter lesions (0.25 mm<sup>2</sup>, Supplementary Figure 1Ba) of GST-pi-stained section, in the white matter of three predefined BrdU, PDGFR- $\alpha$ , and ssDNA sections (bregma +1.60 mm, +0.70 mm, and -0.26 mm; Supplementary Figure 1Bb), and in white matter lesions of autopsy specimens of GST-pi-, PDGFR- $\alpha$ -, and PCNA-positive cells (0.75, 0.75, 1.25 mm<sup>2</sup>, respectively). A one-way ANOVA (analysis of variance) followed by *post hoc* Fisher-protected least significant difference test was used to determine the significant differences in various indices among the groups. A *P*-value of <0.05 was considered statistically significant.

## Results

### Changes in Oligodendrocyte Progenitor Cell and Oligodendrocyte Populations in Human Ischemic White Matter Lesions of Patients with Vascular Dementia

We compared the white matter of five patients with ischemic white matter disease with those of six patients free of such lesions. Figure 1A shows the clinical characteristics of the normal control and patients with white matter lesions. Brain sections prepared by KB staining showed white matter lesions only in patients with ischemic white matter disease (Figures 1Ba and 1Bg). Furthermore, the density of oligodendrocytes positive for GST-pi (a marker of mature oligodendrocyte) and CNPase (a marker of more mature stage of oligodendrocyte) were reduced significantly, whereas the density of cells positive for PDGFR- $\alpha$  (a marker of OPCs) and ssDNA (a marker of cell death) increased signifi-

cantly in the ischemic white matter compared with the control group (Figures 1B and 1C). Cells positive for PCNA (a marker of newly generated cells) were few in the control group, but in significant numbers in the ischemic white matter disease group, which also coexpressed PDGFR- $\alpha$  (Figure 1Da). Furthermore, ssDNA-positive cells coexpressed CNPase (a marker of mature oligodendrocyte; Figure 1Db). These findings suggest that hypoperfusion injury increased the number of OPCs but decreased the number of oligodendrocytes. On the basis of these results, we hypothesized that white matter damage and OPC cell death caused by hypoperfusion could be prevented by promoting normal development of increased OPCs, which in turn increase the number of oligodendrocytes and hence the reconstruction of myelin sheathes.

### Effects of Hypoperfusion on White Matter Lesions in Rodents

We used an animal model of permanent BCCAL (Supplementary Figures 1A and 1B) to study the effect of PDE3 inhibition on restoration of white matter damaged by hypoperfusion in rats. Figure 2A shows representative KB-stained photomicrographs of the white matter. A time-dependent progression of white matter lesions was noted (Figure 2B), and PDE3I significantly decreased the white matter grading score at each time point relative to the vehicle group (Figure 2B). The density of GST-pi-positive cells increased significantly in the vehicle group at 14 days after induced ischemia compared with the sham-operated rats, but then decreased to a density similar to the sham group. However, CNPase-positive cells were decreased in a time-dependent manner. Only a few PDGFR- $\alpha$ -positive cells were found in the white matter of the sham-operated group. In the vehicle group, the number of PDGFR- $\alpha$ -positive cells was significantly higher after 7 days, increased continuously until 28 days. The PDE3I maintained a significantly higher number of GST-pi-positive cells at all time intervals compared with the other groups, and maintained the density of CNPase-positive cells. In PDE3I-treated rats, the number of PDGFR- $\alpha$ -positive cells was significantly higher after 7 days, but it returned to the level observed in the sham-operated rats after 28 days (Figures 2C–2F). Microglia and astrocytes were activated immediately after hypoperfusion; however, such activation was reduced in the PDE3I group compared with the vehicle group (Supplementary Figures 3A and 3B). To evaluate PDE3 expression and its localization in the rat brain, we conducted immunohistochemical analysis. The PDE3 expression was evident in both the cerebral cortex and the white matter region. With regard to PDE3-positive cells detected in the white matter, ~80% coexpressed CNPase and 20% coexpressed NG2. Moreover, some of these cells

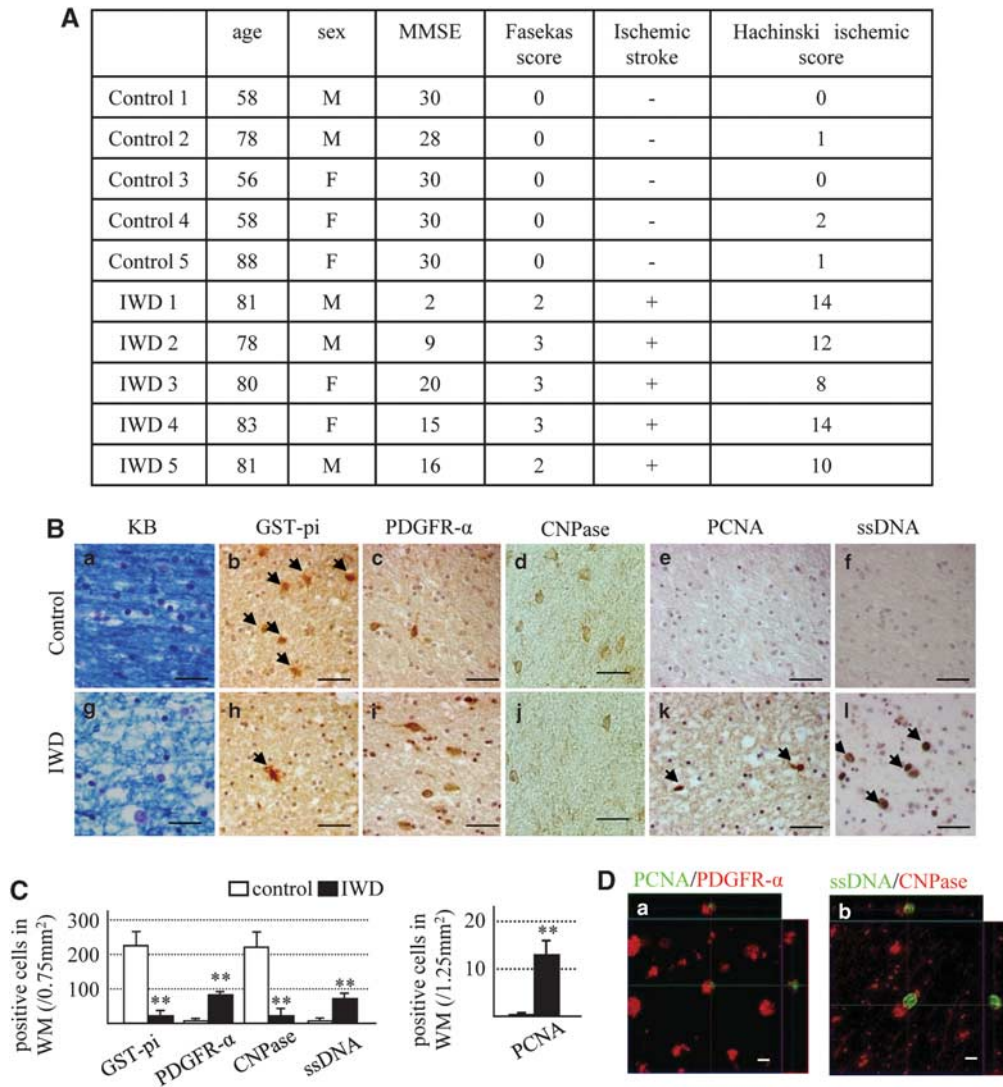


**Figure 1** Human studies. **(A)** Clinical characteristics of the patients and normal control and white matter lesions. MMSE: mini-mental scale (cutoff 24/30). Fazekas score and Hachinski ischemic score were determined on the basis of the methods described by Fazekas *et al* (1988) and Hachinski *et al* (1975). **(B)** Photomicrographs of Klüver–Barrera (a, g)-, GST-pi (b, h; arrowheads, positive cells)-, PDGFR- $\alpha$  (c, i)-, CNPase (d, j)-, PCNA (e, k; arrowheads, positive cells)-, and ssDNA (f, l; arrowheads, positive cells)-stained white matter sections. Control group (a–f) and ischemic white-matter diseases (IWD) group (g–l). Bars = 50  $\mu$ m. **(C)** Number of GST-pi-, PDGFR- $\alpha$ -, CNPase-, and PCNA-positive cells in white matter (WM). Data are mean  $\pm$  s.e.m. of control group ( $n = 6$ ) and ischemic white-matter diseases group ( $n = 5$ ). **(D)** Immunofluorescence staining of PDGFR- $\alpha$  (red)/PCNA (green) (a) and CNPase (red)/ssDNA (green) (b) in the white matter of the ischemic white-matter diseases group of Z-stack images. Bars = 10  $\mu$ m. \*\* $P < 0.001$ , compared with the control group.

also coexpressed CD31 (endothelial cell maker) (Figure 2G).

### Effects of Hypoperfusion on Various Physiologic Parameters and Learning Memory

We next investigated whether BCCAL affects CBF and learning memory and evaluated the effects of PDE3I on these parameters. Cerebral blood flow was measured in bilateral temporal windows by laser Doppler flowmetry before and after BCCAL. No difference of laterality of CBF was evident (data not shown). Furthermore, there was no difference in CBF

between the vehicle group and the PDE3I group throughout the entire study period (left temporal window; Figure 3A).

Next, we conducted the Morris water-maze task to evaluate learning memory. Before BCCAL, all rats escaped the water maze in  $< 20$  secs. After BCCAL, the vehicle group showed significantly longer escape latency than did the sham group. Interestingly, the escape latency of the PDE3I group gradually decreased over the testing period compared with the vehicle group (Figure 3B).

PDE3I is known to increase intracellular cAMP contents (Choi *et al*, 2002). Accordingly, we checked cAMP level in the white matter. The cAMP content

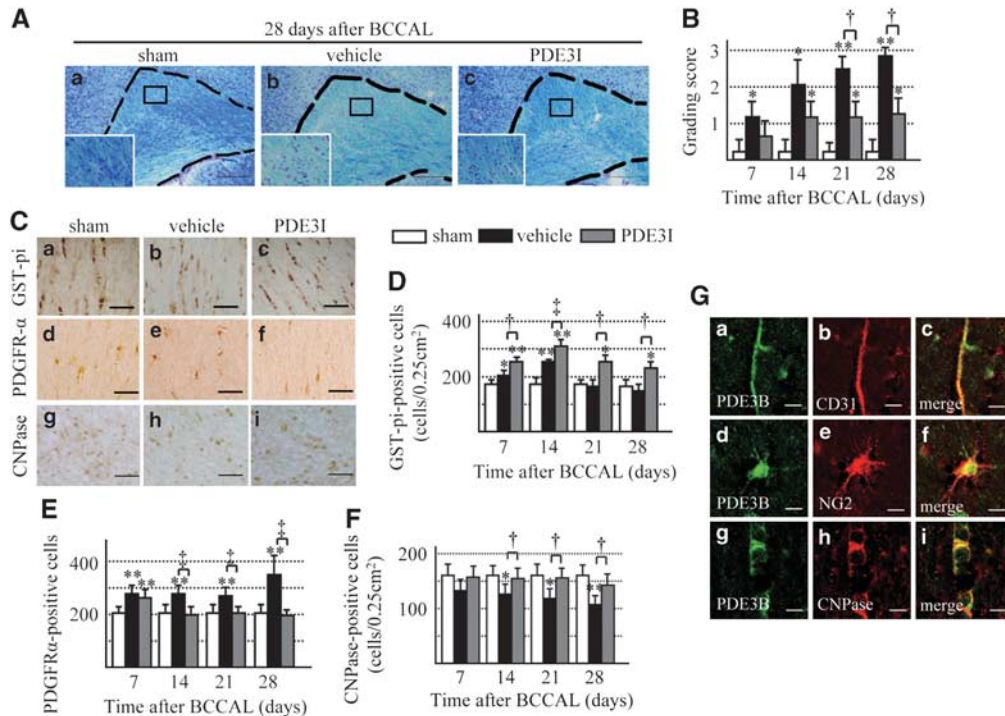


**Figure 2** (A) Photomicrographs of Klüver–Barrera-stained sections of the experimental rat white matter (marked by dotted line). Sham (a), vehicle (b), and PDE31 (c) at 28 days after BCCAL. Insets: magnified views. Magnification,  $\times 100$ . Bar =  $150\ \mu\text{m}$ . (B) Grading-score histograms of the sham, vehicle, and PDE31 white-matter lesion groups. (C) Photomicrographs of GST-pi (a–c)-, PDGFR- $\alpha$  (d–f)-, and CNPase (g–i)-stained cells in the white matter of sham (a, d, g), vehicle (b, e, h), and PDE31 (c, f, i) groups at 28 days after BCCAL. Bars =  $40\ \mu\text{m}$ . (D–F) Proportion of GST-pi (panel D)-, PDGFR- $\alpha$  (panel E)-, and CNPase (panel F)-positive cells in the white matter. (G) Double immunofluorescent staining of PDE3B (green, (a, d, g)), CD31 (red, (b)), CNPase (red, (e)), NG2 (red, (h)), and merged images (c, f, i) in the white matter of sham group. Bars =  $10\ \mu\text{m}$ . Values are mean  $\pm$  s.e.m. of 5 rats in each group. \* $P < 0.05$ , \*\* $P < 0.001$ , compared with the sham-operated group; † $P < 0.05$ , †† $P < 0.001$ , compared with the vehicle group.

was significantly lower in the vehicle group than in the sham group at 14 days after hypoperfusion, and continued to decrease thereafter in a time-dependent manner. In contrast, cAMP levels were maintained at all time intervals in the PDE31 group. (Figure 3C). Cyclic AMP manages various neurotrophic factors through CREB in oligodendrocytes or their progenitors (Saini *et al*, 2004; Shiga *et al*, 2005). Therefore, we evaluated the expression of pCREB by immunohistochemistry. The number of pCREB-positive cells in the white matter decreased after BCCAL in a time-dependent manner in the vehicle and cilostazol groups, although this was more prominent in the former group. Double staining showed that pCREB was coexpressed with CNPase in  $\sim 80\%$  of the cells and with NG2 in  $\sim 20\%$  of the cells (Figures 3D–3F). The above results indicate that ischemic insult results in increased numbers of immature and mature oligodendrocytes, but decreased more mature oligodendrocytes and that cerebral hypoperfusion affects learning memory. In addition, PDE31 protects against progression of white matter lesion and impairment of learning memory. These effects were also followed by an increase in intracellular cAMP, leading to restoration of CREB activation in the white matter lesion.

### Changes in the Proportion of Bromodeoxyuridine-Labeled Cells

The BrdU-labeled cells were detected not only in the white matter area but also in the subventricular zone (data not shown). We determined cell proliferation in the white matter after ischemia by counting the number of BrdU-positive cells at several time points (Supplementary Figure A). A few BrdU-labeled cells were found in the white matter of sham-operated control brains (Figure 4Aa). In the vehicle group, the number of BrdU-labeled cells significantly increased after 14 days and continued to increase until 28 days, compared with the sham group (Figures 5Ab and 5B). In contrast, in the PDE31-treated group, the maximum number of BrdU-labeled cells was observed after 7 days, decreased after 14 days, and remained at that level after 28 days, compared with the sham group (Figures 4Ac and 4Ba). PDE31 treatment enhanced cell survival rate of newly generated BrdU-labeled cells compared with the vehicle group (Figure 4Bb).

To identify the type of BrdU-expressing cells, double immunofluorescence labeling was performed, and a series of glial markers were used to identify oligodendrocytes (GST-pi, CNPase), OPCs

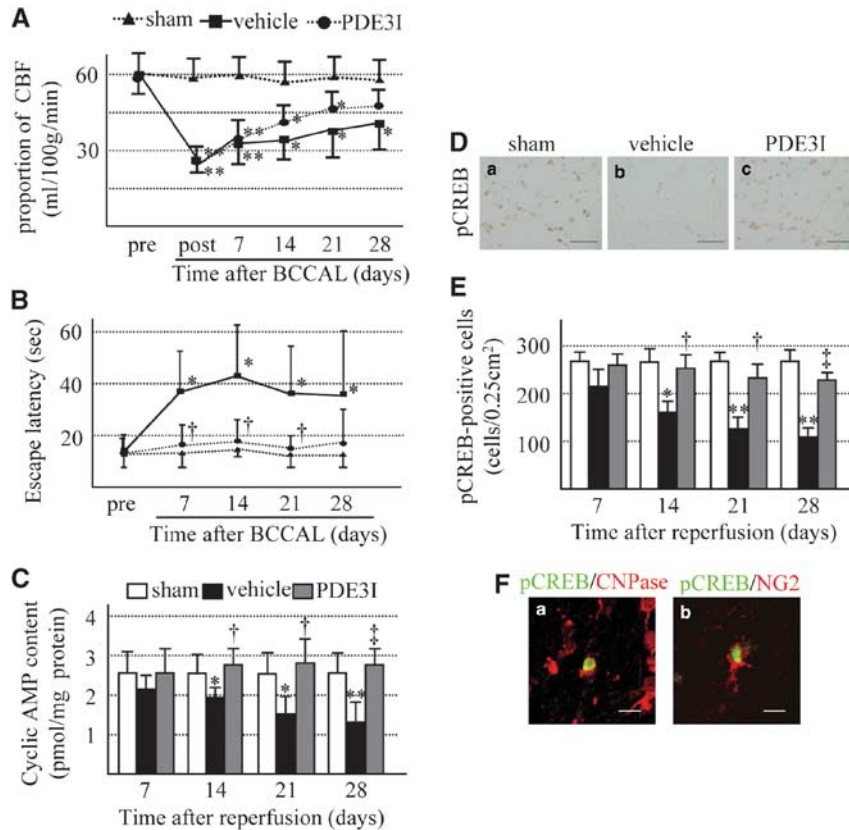


**Figure 3** (A) Temporal changes in cerebral blood flow (CBF). Pre: before BCCAL; post: immediately after BCCAL, and at 7, 14, 21, and 28 days after BCCAL. (B) Effect of ischemic insult on learning deficit as measured by the Morris water-maze task. (C) cAMP content of white matter. (D) Photomicrographs of pCREB-stained cells in the white matter of sham (a), vehicle (b), and PDE3I (c) groups at 28 days after BCCAL. Bars = 40  $\mu$ m. (E) Proportion of pCREB-positive cells in the white matter. (F) Double immunofluorescent staining of pCREB (green), CNPase (red, a) and NG2 (red, b). Bars = 10  $\mu$ m. Values are mean  $\pm$  s.e.m. of 5 rats in each group. \* $P$  < 0.05, \*\* $P$  < 0.001 compared with the sham-operated group; † $P$  < 0.05, ‡ $P$  < 0.001 compared with the vehicle group.

(PDGFR- $\alpha$ ), and astrocytes (GFAP). In all groups, there were only few BrdU/GFAP and BrdU/GST-pi double-positive cells, but the remaining cells were BrdU/PDGFR- $\alpha$  double positive. At 14  $\rightarrow$  21d, the proportion of GST-pi/BrdU and CNPase/BrdU double-positive cells increased significantly, whereas that of PDGFR- $\alpha$ /BrdU double-positive cells decreased significantly in the white matter of PDE3I-treated rats compared with the vehicle group (Figures 4C and 4D). These results show that ischemic insult promotes the newly generated OPCs despite progression of the white matter lesion, and that PDE3I promotes the differentiation and survival of newly generated OPCs.

### Changes in the Proportion of ssDNA-Positive Cells

In the vehicle group, the number of ssDNA-positive cells increased significantly after 7 days and continued to increase until day 28 compared with the sham group (Figures 5A and 5B). In contrast, the number of ssDNA-positive cells also increased in the PDE3I group compared with the sham group, but

there were significantly fewer ssDNA-positive cells relative to the vehicle group (Figures 5A and 5C).

To identify the type of ssDNA-positive cells, we carried out double immunofluorescence studies using cell-type markers that identify oligodendrocyte (CNPase), OPCs (NG2), astrocytes (GFAP), and newly formed cells (BrdU). In all groups, ssDNA-positive cells were colocalized with CNPase (Figure 5B). Some of the ssDNA-positive cells were also colocalized with NG2-positive cells (Supplementary Figure 3C). At 14  $\rightarrow$  21d, a significantly higher proportion of BrdU/ssDNA-double positive cells was observed in the vehicle group than in the PDE3I group (Figure 5D). These results suggest that PDE3I has an important role in OPC differentiation and prevents cell death.

### Changes in Enhanced Green Fluorescent Protein-Labeled Cells

Using EGFP-retrovirus labeling, we investigated whether the newly formed OPCs participate in myelination during posthypoperfusion (Figure 6A). As GFP labeling fills the cell processes, we were able to identify two subtypes of oligodendrocytes on the

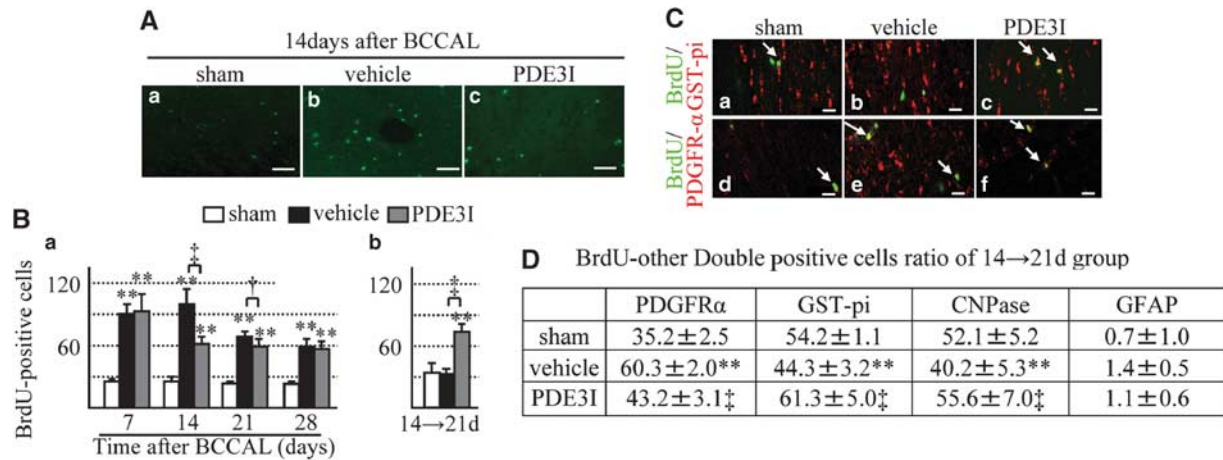


**Figure 4** (A) 5-Bromodeoxyuridine (BrdU) immunofluorescence staining in the white matter of vehicle- and PDE3I-treated rats. Sham (a), vehicle (b), and PDE3I (c) rats at day 14 after BCCAL. Bar = 50  $\mu$ m. (B) Number of BrdU-positive cells in the white matter. (C) Double immunofluorescent staining of BrdU, GST-pi, and PDGFR- $\alpha$ . Representative white matter of the sham, vehicle-, and PDE3I-treated groups at 14 days after BCCAL (green, BrdU; red, GST-pi (a–c); PDGFR- $\alpha$  (d–f); a, d; sham; b, e; vehicle; and c, f; PDE3I group, arrowheads; merged cells). Scale bar = 20  $\mu$ m. (D) Proportion of BrdU-positive cells double-labeled with glial cell markers (PDGFR- $\alpha$ , GST-pi, CNPase, and GFAP) in white matter. Data in panel B and D are mean  $\pm$  s.e.m. of 5 rats in each group. \* $P$  < 0.05, \*\* $P$  < 0.001, compared with the sham-operated group; † $P$  < 0.05, ‡ $P$  < 0.001, compared with the vehicle group.

basis of the morphologic characteristics reported previously (Menn *et al*, 2006) i.e., mature myelinating oligodendrocytes (Figure 6Cd) and highly branched cells with a morphology typical of parenchymal OPCs, also known as nonmyelinating oligodendrocytes (Figure 6Ce). Enhanced green fluorescent protein-positive cells coexpressed mainly PDGFR- $\alpha$  at 72 h after virus injection (Figures 6B and 6D). However, 14 days after hypoperfusion, abundant EGFP-positive cells with linear processes, which are morphologically myelinating cells (Figure 6Cd, arrows), were noted in the PDE3I groups as well as in the sham group, and coexpressed mainly GST-pi. In the vehicle group, there were only a few EGFP-positive cells that coexpressed GST-pi; instead, the EGFP-positive cells were colocalized mainly with PDGFR- $\alpha$  cells (Figures 6C and 6D). These data were similar to those of the BrdU-labeling experiment and the majority of the dendrite-like structures were merged with myelin basic protein (Figure 6E, arrows), indicating that the newly generated oligodendrocytes participate in remyelination of the white matter lesion and that this process is also enhanced by administration of PDE3I after chronic cerebral hypoperfusion.

#### Effects of Inhibition of Protein Kinase A and C

PDE III inhibition can be modulated by pharmacological or physiologic activators of protein kinase C (Raychowdhury *et al*, 2002) and protein kinase A (Soto *et al*, 2006). In the next series of experiments, rats were subjected to BCCAL followed by a 14-day treatment with PDE3I. On day 7 after BCCAL, they were injected with BrdU and H7, a novel protein

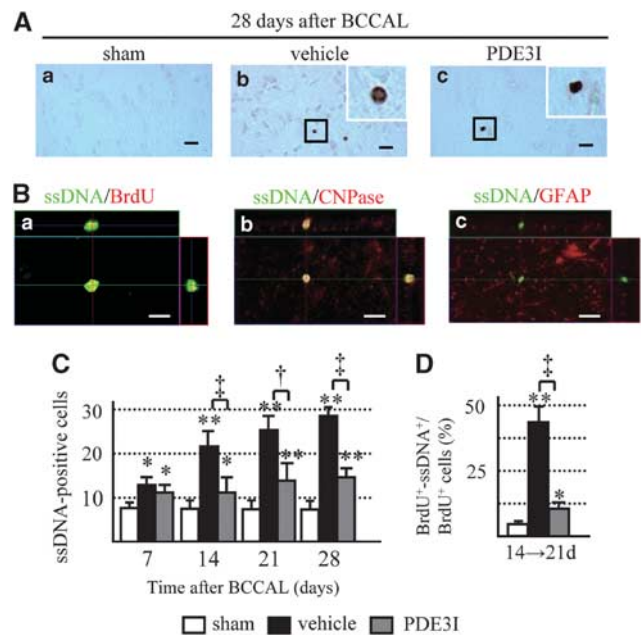


**Figure 5** (A) Photomicrographs showing ssDNA staining in the white matter of sham (a), vehicle (b)-, and PDE3I (c)-treated rats 28 days after BCCAL. Bar = 20  $\mu$ m. Insets in b and c: magnified views. Magnification,  $\times$  400. (B) Colocalization of ssDNA-positive cells in the vehicle group at days 14→21 after BCCAL. (C) Number of ssDNA-positive cells. Double immunofluorescence BrdU staining (red (a)), CNPase (red (b)), GFAP (red (c)), and ssDNA (green (a–c)). Bar = 10  $\mu$ m. (D) Percentage of BrdU/ssDNA-double-positive cells relative to BrdU-positive cells. BrdU<sup>+</sup>: BrdU-positive cells, ssDNA<sup>+</sup>: ssDNA-positive cells. Data in panels B and D are mean  $\pm$  s.e.m. of 5 rats in each group. \* $P$  < 0.05, \*\* $P$  < 0.001, compared with sham-operated group; † $P$  < 0.05, ‡ $P$  < 0.001, compared with vehicle group.



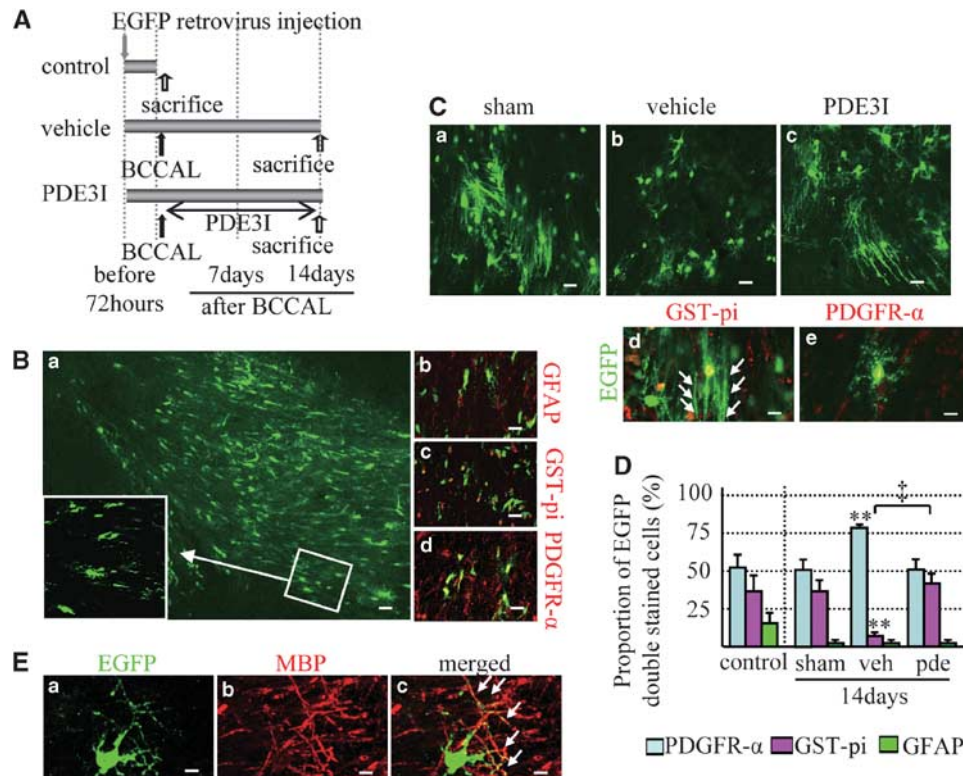


**Figure 6** (A) EGFP-retrovirus injection protocol (sham,  $n = 4$ ; vehicle,  $n = 6$ ; cilostazol,  $n = 4$ ). (B) (a) Photomicrographs showing GFP staining in the white matter 72 h after injection. Bar = 40  $\mu\text{m}$ . (b–d) Colocalization of GFP-positive cells in the white matter 72 h after injection (red, b; GFAP, c; GST-pi, d; PDGFR- $\alpha$ ). Bars = 20  $\mu\text{m}$ . (C) GFP immunofluorescence staining in the white matter of sham (a), vehicle (b)-, and PDE3I (c)-treated rats at day 14 after BCCAL. Bars = 20  $\mu\text{m}$ . Double immunofluorescence staining for GST-pi (red (d)), PDGFR- $\alpha$  (red (e)), GFP (green (d, e)). Bars = 10  $\mu\text{m}$ . (D) Proportion of GFP-positive cells double labeled with glial cell markers (PDFGR- $\alpha$ , GST-pi, and GFAP) in the white matter of sham, sham-operated group; veh, vehicle group; pde, PDE3I-treated group. Data are mean  $\pm$  s.e.m.  $**P < 0.001$ , compared with the sham-operated group;  $^{\ddagger}P < 0.001$ , compared with the vehicle group. (E) Colocalization of GFP-positive cells in the white matter of PDE3I group at day 14 after BCCAL. Double immunofluorescence staining for GFP (green (a)), MBP (red (b)), and merged (yellow (c), arrowheads; merged dendrites). Bar = 10  $\mu\text{m}$ .

kinase A/protein kinase C inhibitor. The H7 was administered into the lateral ventricle at a rate of 10 nmol/ $\mu\text{L}$  per h using an osmotic mini pump. Control rats received PDE3I + saline (Figure 7A). This dose was based on preliminary experiments that found no changes in white matter and cell count of the sham group. All rats were sacrificed on day 14.

The number of BrdU-positive cells in the PDE3I + H7 group was significantly lower than in the PDE3I + saline group (Figures 7Ba–7Bc). Moreover, only a few BrdU/GST-pi-positive cells but abundant BrdU/PDGFR- $\alpha$ -positive cells were identified in the PDE3I + H7 group, compared with the PDE3I + saline group (Figure 7Bd). Thus, the proportion of BrdU-positive cells coexpressing BrdU/GST-pi and PDGFR- $\alpha$  was significantly different in the PDE3I + H7 group than in the PDE3I + saline group (Figure 7Bd).

Klüver–Barrera staining showed worsening of white matter lesions in the PDE3I + H7 group compared with the PDE3I + saline group (Figure 7C). Moreover, the proportion of GST-pi- and CNPase-positive cells (oligodendrocyte) decreased significantly, whereas the proportion of PDGFR- $\alpha$ -

positive cells (OPCs) and ssDNA-positive cells (apoptotic cells) increased significantly in H7-treated rats, relative to the PDE3I + saline group (Figure 7D). Treatment with protein kinase C/protein kinase A inhibitor in the vehicle group (no treatment with PDEIII inhibitor) resulted in progression of the white matter lesion, reduction in BrdU-positive cells and GST-pi-positive cells, and increased PDGFR- $\alpha$ -positive cells at 7 days after H7 treatment, compared with without H7 (vehicle group). However, the proportion of BrdU/other glial cells-double positive cells was not significantly different between the vehicle and vehicle + H7 groups (Supplementary Figure 2). These results suggest that inhibition of PDE III has an important role in OPC differentiation and prevention of cell death induced by cerebral hypoperfusion.

## Discussion

In this study, we analyzed the mechanisms of tissue repair in white matter lesions in humans and in a rodent model of chronic cerebral hypoperfu-

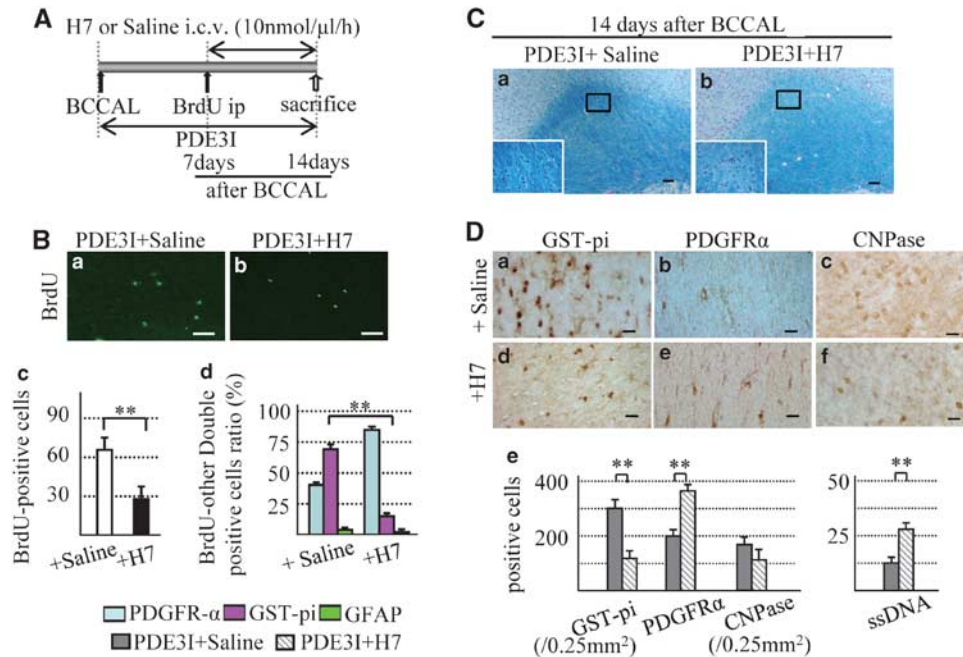


**Figure 7** (A) Osmotic mini-pump protocol. (B) a, b; 5-bromodeoxyuridine (BrdU) immunofluorescence staining in the white matter of PDE3I + Saline group (a) and + H7 group (b) 14 days after BCCAL. Bars = 50  $\mu$ m. (c) Number of BrdU-positive cells in the white matter. (d) Proportion of BrdU-positive cells double labeled with glial cell markers (PDFGR- $\alpha$ , GST-pi, and GFAP). (C) Photomicrographs of Klüver–Barrera staining of the white matter of PDE3I + Saline (a) and PDE3I + H7 group (b) at 14 days after BCCAL. (D) Photomicrographs of GST-pi (a, d) and PDGFR- $\alpha$  (b, e), CNPase (c, f) in white matter of the PDE3I + Saline (a–c) and PDE3I + H7 (d–f) groups 14 days after BCCAL. Bars = 20  $\mu$ m. (E) Proportion of GST-pi-, PDGFR- $\alpha$ -, CNPase- and ssDNA-positive cells in the white matter. Data in Bc and De are mean  $\pm$  s.e.m. of 5 rats in each group, \* $P$  < 0.05; \*\* $P$  < 0.001 compared with the other groups.

sion. The major findings were that chronic cerebral hypoperfusion resulted in a transient increase in oligodendrocyte progenitors, which subsequently resulted in cell death. PDE3I treatment promoted the differentiation and survival of newly generated oligodendrocytes, which resulted in enhanced remyelination followed by functional recovery.

Demyelination and loss of oligodendrocytes are pathologic hallmarks of ischemic white matter disease, which is associated with vascular dementia (Jellinger, 2007). The number of oligodendrocytes in the deep white matter is reduced by ~50% in patients with vascular dementia (Yamanouchi, 1991). An increase in the apoptosis frequency of oligodendrocytes is a major histologic correlate of white matter lesions (Brown *et al*, 2000), indicating that the loss of oligodendrocytes is involved in demyelination and reduction in nerve fibers that lead to cognitive decline. However, there is little or no information regarding the endogenous repair mechanisms of ischemic white matter lesions in the adult mammalian brain. Our findings showed enhanced cell proliferation and OPC generation in white matter lesions both in the rodent and the human CNS under chronic ischemia. Similar pathologic changes have been described in multiple sclerosis (Chang *et al*, 2002; Niehaus *et al*, 2000; Prineas *et al*, 1993;

Wolswijk, 1998). Studies of multiple sclerosis suggest at least two types of lesions in which remyelination eventually fails; those in which OPCs are present in insufficient numbers, implying failure of survival or recruitment (Niehaus *et al*, 2000; Prineas *et al*, 1993), and those in which OPCs are present but are unable to complete myelination (Chang *et al*, 2002; Wolswijk, 1998). Whereas our data showed that new OPCs regenerated abundantly immediately after ischemia, but these cells underwent cell death or were unable to differentiate to mature oligodendrocytes for remyelination, suggesting that the regenerative process can occur in the CNS but fail to result in the restoration of brain function. Treatment with PDE3I ameliorated these negative effects of cerebral hypoperfusion through restoration of intracellular cAMP and subsequent CREB activation. Previous data also highlighted the importance of the CREB signaling pathway in the differentiation and survival of oligodendrocyte progenitors (Saini *et al*, 2004; Shiga *et al*, 2005). Considered together, these results emphasize the potential benefits of PDE3I in patients with vascular dementia as it enhances oligodendrogenesis and remyelination of injured white matter regions.

To our knowledge, this is the first study to show that BCCAL results in the stimulation of cell proliferation and generation of oligodendrocyte

lineage in white matter lesions, followed by adult mammalian brain repair. Previous studies have reported that stroke results in increased cell proliferation and neuroblasts generation in the subventricular zone followed by migration of newly formed neuroblasts into the damaged striatum (Arvidsson *et al*, 2002). Furthermore, OPCs derived from the subventricular zone migrate to the demyelinated lesions and participate in myelin repair in the adult brain (Menn *et al*, 2006). These results support the notion that new neurons and glial cells can potentially repair the degenerated adult CNS tissue and regain the lost function. The results of our study showed that BCCAL resulted in an increase in the number of BrdU-positive cells in the white matter, whereas PDE3I decreased their number. However, PDE3I increased the proportion of BrdU/GST-pi cells and kept the number of CNPase-positive cells, which represent more advanced-stage oligodendrocytes, and decreased cell death. Using EGFP labeling, we also showed the maturation of oligodendrocyte lineage; we believe that these labeled oligodendrocytes participate in the restoration of white matter lesion. As there was slight improvement in CBF in the PDE3I treatment group compared with vehicle group, we could not exclude possible changes in perfusion in the deep white matter. In this regard, further study could be required to explore the possible association between CBF changes and tissue repair.

Previous reports have shown that EGFP labeling, which fills the cell processes, allows the identification of two subtypes of oligodendrocytes on the basis of morphology: mature myelinating oligodendrocytes (Butt, 2004; Levison and Goldman, 1993) and highly branched cells with a typical morphology of parenchymal OPCs, also known as nonmyelinating oligodendrocytes (Butt, 2004). Proliferating oligodendrocyte progenitors are present in the adult brain parenchyma, including the white matter (Polito and Reynolds, 2005). In our study, injection of retrovirus encoding EGFP into the white matter resulted in labeled myelinating and nonmyelinating oligodendrocytes 7 days later. Furthermore, myelinating oligodendrocytes were detected only in the sham and PDE3I groups, but not in the vehicle group. These results suggest that PDE3I affects not only cell survival but also differentiation and maturation of newly generated OPCs, leading to remyelination.

In conclusion, this study showed that the mechanisms involved in the regulation of survival and differentiation of OPCs have an important role in white matter tissue regeneration in rats after bilateral carotid artery occlusion. Although further studies are required to investigate several issues in this model such as the other effects on neurogenesis of the subventricular zone, the present results suggest that PDE3I is potentially beneficial therapeutically on the basis of its regenerative effects, and may be useful in the treatment of patients with poststroke complications by protecting against the progression of white matter lesions in ischemic cerebrovascular disease.

## Acknowledgements

Cilostazol was a kind gift from Otsuka Pharmaceutical Co., Ltd., Tokyo, Japan.

## Conflict of interest

The authors declare no conflict of interest.

## References

- Arvidsson A, Collin T, Kirik D, Kokaia Z, Lindvall O (2002) Neuronal replacement from endogenous precursors in the adult brain after stroke. *Nat Med* 8:963–70
- Bansal R, Pfeiffer SE (1997) FGF-2 converts mature oligodendrocytes to a novel phenotype. *J Neurosci Res* 50:215–28
- Barnett AH, Bradbury AW, Brittenden J, Crichton B, Donnelly R, Homer-Vanniasinkam S, Mikhailidis DP, Stansby G (2004) The role of cilostazol in the treatment of intermittent claudication. *Curr Med Res Opin* 20:1661–70
- Brown WR, Moody DM, Thore CR, Challa VR (2000) Cerebrovascular pathology in Alzheimer's disease and leukoariosis. *Ann N Y Acad Sci* 903:39–45
- Butt AM (2004) *Structure and Function of Oligodendrocytes*. New York, USA: Oxford University Press
- Chang A, Tourtellotte WW, Rudick R, Trapp BD (2002) Premyelinating oligodendrocytes in chronic lesions of multiple sclerosis. *N Engl J Med* 346:165–73
- Choi JM, Shin HK, Kim KY, Lee JH, Hong KW (2002) Neuroprotective effect of cilostazol against focal cerebral ischemia via antiapoptotic action in rats. *J Pharmacol Exp Ther* 300:787–93
- Fazekas F, Niederkorn K, Schmidt R, Offenbacher H, Horner S, Bertha G, Lechner H (1988) White matter signal abnormalities in normal individuals: correlation with carotid ultrasonography, cerebral blood flow measurements, and cerebrovascular risk factors. *Stroke* 19:1285–8
- Gensert JM, Goldman JE (1997) Endogenous progenitors remyelinate demyelinated axons in the adult CNS. *Neuron* 19:197–203
- Gerlai R (2001) Behavioral tests of hippocampal function: simple paradigms complex problems. *Behav Brain Res* 125:269–77
- Hachinski VC, Iliff LD, Zilhka E, Du Boulay GH, McAllister VL, Marshall J, Russell RW, Symon L (1975) Cerebral blood flow in dementia. *Arch Neurol* 32:632–7
- Ihara M, Tomimoto H, Kinoshita M, Oh J, Noda M, Wakita H, Akiguchi I, Shibasaki H (2001) Chronic cerebral hypoperfusion induces MMP-2 but not MMP-9 expression in the microglia and vascular endothelium of white matter. *J Cereb Blood Flow Metab* 21:828–34
- Jellinger KA (2007) The enigma of vascular cognitive disorder and vascular dementia. *Acta Neuropathol* 113:349–88
- Lee JH, Shin HK, Park SY, Kim CD, Lee WS, Hong KW (2009) Cilostazol preserves CA1 hippocampus and enhances generation of immature neuroblasts in dentate gyrus after transient forebrain ischemia in rats. *Exp Neurol* 215:87–94

- Levison SW, Goldman JE (1993) Both oligodendrocytes and astrocytes develop from progenitors in the subventricular zone of postnatal rat forebrain. *Neuron* 10:201–12
- Liu J, Bartels M, Lu A, Sharp FR (2001) Microglia/macrophages proliferate in striatum and neocortex but not in hippocampus after brief global ischemia that produces ischemic tolerance in gerbil brain. *J Cereb Blood Flow Metab* 21:361–73
- Mabuchi T, Kitagawa K, Ohtsuki T, Kuwabara K, Yagita Y, Yanagihara T, Horii M, Matsumoto M (2000) Contribution of microglia/macrophages to expansion of infarction and response of oligodendrocytes after focal cerebral ischemia in rats. *Stroke* 31:1735–43
- Matsumoto M (2005) Cilostazol in secondary prevention of stroke: impact of the Cilostazol Stroke Prevention Study. *Atheroscler Suppl* 6:33–40
- Menn B, Garcia-Verdugo JM, Yaschine C, Gonzalez-Perez O, Rowitch D, Alvarez-Buylla A (2006) Origin of oligodendrocytes in the subventricular zone of the adult brain. *J Neurosci* 26:7907–18
- Niehaus A, Shi J, Grzenkowski M, Diers-Fenger M, Archelos J, Hartung HP, Toyka K, Bruck W, Trotter J (2000) Patients with active relapsing-remitting multiple sclerosis synthesize antibodies recognizing oligodendrocyte progenitor cell surface protein: implications for remyelination. *Ann Neurol* 48:362–71
- Polito A, Reynolds R (2005) NG2-expressing cells as oligodendrocyte progenitors in the normal and demyelinated adult central nervous system. *J Anat* 207:707–16
- Prineas JW, Barnard RO, Revesz T, Kwon EE, Sharer L, Cho ES (1993) Multiple sclerosis. Pathology of recurrent lesions. *Brain* 116(Pt 3):681–93
- Raychowdhury R, Schafer G, Fleming J, Rosewicz S, Wiedenmann B, Wang TC, Hocker M (2002) Interaction of early growth response protein 1 (Egr-1), specificity protein 1 (Sp1), and cyclic adenosine 3′/5′-monophosphate response element binding protein (CREB) at a proximal response element is critical for gastrin-dependent activation of the chromogranin A promoter. *Mol Endocrinol* 16:2802–18
- Redwine JM, Armstrong RC (1998) In vivo proliferation of oligodendrocyte progenitors expressing PDGF $\alpha$ R during early remyelination. *J Neurobiol* 37:413–28
- Reynolds R, Hardy R (1997) Oligodendroglial progenitors labeled with the O4 antibody persist in the adult rat cerebral cortex in vivo. *J Neurosci Res* 47:455–70
- Roman GC, Tatemichi TK, Erkinjuntti T, Cummings JL, Masdeu JC, Garcia JH, Amaducci L, Orgogozo JM, Brun A, Hofman A *et al.* (1993) Vascular dementia: diagnostic criteria for research studies. Report of the NINDS-AIREN International Workshop. *Neurology* 43:250–60
- Saini HS, Gorse KM, Boxer LM, Sato-Bigbee C (2004) Neurotrophin-3 and a CREB-mediated signaling pathway regulate Bcl-2 expression in oligodendrocyte progenitor cells. *J Neurochem* 89:951–61
- Shiga H, Yamane Y, Kubo M, Sakurai Y, Asou H, Ito E (2005) Differentiation of immature oligodendrocytes is regulated by phosphorylation of cyclic AMP-response element binding protein by a protein kinase C signaling cascade. *J Neurosci Res* 80:767–76
- Soto I, Rosenthal JJ, Blagburn JM, Blanco RE (2006) Fibroblast growth factor 2 applied to the optic nerve after axotomy up-regulates BDNF and TrkB in ganglion cells by activating the ERK and PKA signaling pathways. *J Neurochem* 96:82–96
- Suzuki A, Obi K, Urabe T, Hayakawa H, Yamada M, Kaneko S, Onodera M, Mizuno Y, Mochizuki H (2002) Feasibility of ex vivo gene therapy for neurological disorders using the new retroviral vector GCDNsap packaged in the vesicular stomatitis virus G protein. *J Neurochem* 82:953–60
- Tanaka K, Nogawa S, Ito D, Suzuki S, Dembo T, Kosakai A, Fukuuchi Y (2001) Activation of NG2-positive oligodendrocyte progenitor cells during post-ischemic reperfusion in the rat brain. *Neuroreport* 12:2169–74
- Wakita H, Tomimoto H, Akiguchi I, Kimura J (1994) Glial activation and white matter changes in the rat brain induced by chronic cerebral hypoperfusion: an immunohistochemical study. *Acta Neuropathol* 87:484–92
- Wakita H, Tomimoto H, Akiguchi I, Lin JX, Miyamoto K, Oka N (1999) A cyclooxygenase-2 inhibitor attenuates white matter damage in chronic cerebral ischemia. *Neuroreport* 10:1461–5
- Watanabe T, Zhang N, Liu M, Tanaka R, Mizuno Y, Urabe T (2006) Cilostazol protects against brain white matter damage and cognitive impairment in a rat model of chronic cerebral hypoperfusion. *Stroke* 37:1539–45
- Wolswijk G (1998) Chronic stage multiple sclerosis lesions contain a relatively quiescent population of oligodendrocyte precursor cells. *J Neurosci* 18:601–9
- Wolswijk G, Noble M (1989) Identification of an adult-specific glial progenitor cell. *Development* 105:387–400
- Yamanouchi H (1991) Loss of white matter oligodendrocytes and astrocytes in progressive subcortical vascular encephalopathy of Binswanger type. *Acta Neurol Scand* 83:301–5

Supplementary Information accompanies the paper on the Journal of Cerebral Blood Flow & Metabolism website (<http://www.nature.com/jcbfm>)